

# Intensity Dynamics in a Waveguide Array Laser

Matthew O. Williams and J. Nathan Kutz \*

*Abstract*—The intensity dynamics of a five-emitter laser array subject to a linearly decreasing injection current are examined numerically. We have matched the results of the numerical model to an experimental AlGaAs quantum-dot array laser and have achieved the same robust oscillatory power output with a nearly  $\pi$  phase shift between emitters that was observed in experiments. Due to the linearly decreasing injection current, the output power of the waveguide decreases as a function of waveguide number. For injection currents ranging from 380 to 500 mA, the oscillatory behavior persists with only a slight change in phase difference. However, the fundamental frequency of oscillation increases with injection current, and higher harmonics as well as some fine structures are produced.

*Keywords:* Waveguide arrays, semiconductor lasers

## 1 Introduction

Semiconductor laser arrays have been proposed as a method for achieving increased optical power output [1–4]. This approach has met with mixed results, as standard index guided arrays tend to favor the out-of-phase state as shown by Botez et al [5]. In addition, spatial hole burning and other physical phenomena make achieving a phase-locked device difficult to obtain in practice. Yet, the same nonlinear effects which destroy the phase-locked state can give rise to a variety of dynamical behaviors. Rahman, Winful, and others have shown that the types of unstable array operations includes chaos and sustained oscillations [2, 3]. We explore numerically a five-element array operating in the oscillatory regime with an uneven injection current. The application of Winful’s model to such a device produces results which are consistent with experimental results from an AlGaAs quantum-dot array operating in the same regime. Of particular interest is the frequency of oscillation, as a potential uses of this sort of array is as an all-optical GHz oscillator for photonic integrated circuits.

The model of the array dynamics involves the coupling of the optical field to the carrier density dynamics. This model is derived from a simplification of Maxwell’s wave equation where a TE mode, the slowly varying envelope

approximation, and the effective index approximation are made in succession [6]. Additionally, it is assumed that the charge carrier density is uniform in the direction of propagation. Overall, this model includes the effects of evanescent coupling between waveguide, stimulated emission and absorption, spatial diffraction, carrier antiguiding, losses due to the cladding, and losses due to reflections off the edges of the crystal. The carrier dynamics are influenced by current injection, stimulated and spontaneous emission and absorption, as well as spatial diffusion. Overall, this model is able to reproduce the same dynamics observed in cases of smaller arrays. Additionally, there is good agreement between this model and experimental results in such a five-emitter AlGaAs array.

## 2 Governing Equations

The evolution of the optical field is a combination of guided mode propagation, coupling between guided modes, and pumping or loss due to charge carrier dynamics [3]. Where the effects of charge carrier dynamics to be discounted, the laser could be thought of as a simple dielectric waveguide, and the evolution could be modeled by considering each cold-cavity supermode, the eigenfunctions of the now linear operator, separately. The mechanism for coupling between the various cold-cavity supermodes is the charge carrier dynamics, which introduce nonlinearities that couple these modes to produce additional dynamics not seen in the linear case. Due to importance of nonlinearities, the optical field and carrier dynamics are solved in PDE form given by

$$\frac{\partial U}{\partial \tau} = iC\Delta\eta_{\text{eff}} + (1 - iR)UV + iL_p^2 \frac{\partial^2 U}{\partial x^2} \quad (1a)$$

$$T \frac{\partial V}{\partial \tau} = p(x) - V - (1 + 2V)|U|^2 + L_e^2 \frac{\partial^2 V}{\partial x^2}, \quad (1b)$$

where  $U$  is the envelope of the electric field,  $V$  is the charge carrier density,  $\tau$  is nondimensionalized time, and  $x$  is the spatial dimension, which retains units of microns. The following scalings relate the nondimensional quantities to physical quantities:  $U = (\eta_e^2 g \tau_s / 2c \eta_a)^{1/2} \psi$ ,  $V = \frac{1}{2} g \tau_p (N - N_{\text{th}})$ ,  $p(x) = \frac{1}{2} g \tau_p [j(x) \tau_s - N_{\text{th}}]$ ,  $T = \tau_s / \tau_p$ ,  $g = \Gamma a c \eta_a / \eta_e^2$ ,  $1/\tau_p = (c/\eta_e)[(\eta_c/\eta_e)(1 - \Gamma)\alpha_c + (2/L) \ln(1/r)]$ ,  $N_{\text{th}} = N_0 + 1/g\tau_p$ ,  $L_p = (c\tau_p/2\eta_e^2 k_0)^{1/2}$ ,  $C = \Gamma c k_0 \eta_a \tau_p / \eta_e^2$ , and  $\tau = t/\tau_p$ . In these equations,  $\psi$  is the envelope of the complex electric field in the transverse direction and  $N$  is the charge carrier density. The other

\*Matthew O. Williams and J. Nathan Kutz are with the Department of Applied Mathematics, University of Washington, Seattle, WA 98195 (email: mowill@amath.washington.edu; kutz@amath.washington.edu).

values are readily obtainable from experiment, tables of material properties, and the effective index method. Typical values used in these numerical experiments are  $L_p \approx 7.5$ ,  $C \approx 8 \times 10^3$ ,  $\tau_p \approx 22$ , and  $T \approx 45$ , but the actual values depend heavily upon the material composition of the waveguide array, thickness and geometry of the active and cladding layers, crystal length, and other parameters. Typical values for different types of arrays may be found in Ref. [3, 7] for AlGaAs and InGaP arrays respectively as well as many other sources.

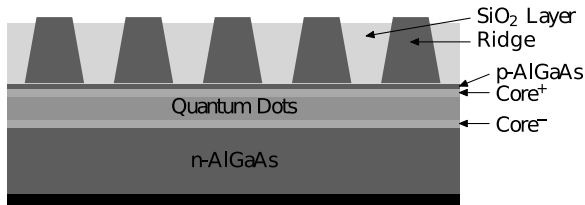


Figure 1: The transverse structure of the five-emitter AlGaAs array being modeled. The model considers five different emitters with sloping sides separated by SiO<sub>2</sub>. The material properties of the array impact the parameters of the model and are thus pertinent even though they do not appear explicitly in the governing equations.

### 3 Lasing Dynamics

The differential equations in (1a) and (1b) are quite general and should apply to any semiconductor array that does not invalidate the assumptions. The particular array of interest is a five-emitter array with a sloping injection current. This can be seen in cross-section in Fig. 1. Physically, the slope of the injection current may be caused by injecting current into all the emitter via one large contact rather than injecting the same current individually into each emitter. Note that this model includes the material properties of the array as they are built-in to the parameters used. The values corresponding to these parameters are shown in Table 1. Note that the listed value of injection current is the sum of the injection current of all five waveguides and not an average value. With these values, the system of equations was evolved in time by use of a time-splitting procedure and transparent boundary conditions [3, 8, 9]. The time-split equations were individually evolved using Crank-Nicolson which is unconditionally stable for diffusion operators such as those in (1).

The parameters of greatest interest are the power output of each emitter and temporal fluctuations of that output. This array, like smaller arrays, is capable of several different dynamical instabilities. One of the first to be examined was the phase-locked state. This has been previously studied in great detail. Like observed by Botez et al., numerical experimentation has shown that the five emitter array also favors the undesirable out-of-

Table 1: Parameter values for a five-emitter AlGaAs waveguide array.

Parameter Description	Symbol	Units	Value
Wavelength	$\lambda$	$\mu\text{m}$	1.178
Ridge Thickness	$W$	$\mu\text{m}$	2.0
Active Layer Thickness	$d$	$\mu\text{m}$	0.4
Cavity Length	$L$	$\mu\text{m}$	4500
Injection Current	$I$	mA	400
Cladding Loss	$\alpha_c$	$\mu\text{m}^{-1}$	$1.0 \times 10^{-3}$
Antiguinding Factor	$R$		3
Carrier Diffusion Length	$L_e$	$\mu\text{m}$	3
Gain Coefficient	$a$		$1.5 \times 10^{-8}$
Active Layer Index	$\eta_a$		3.443
Cladding Layer Index	$\eta_c$		3.12
Effective Index	$\eta_e$		3.386
Insulator Index	$\eta_i$		1.45
Carrier Lifetime	$\tau_s$	ps	2000
Transverse Confinement Factor	$\Gamma$		0.75
End Mirror Reflectivity	$r$		0.53

phase state [5]. Similar to the results of Winful [3], this mode is favored when the separation between waveguides is large and evanescent coupling weak. However, for similar reasons to those given by Winful [10], as the evanescent coupling increasing it begins to overwhelm the system's ability to maintain a steady state causing a phase shift that leads to dynamics.

As coupling increases, it alters the system dynamics creating a series of sustained stable periodic oscillations. As small perturbations off of the theoretical steady state, such as those caused by the error in numerical solvers, produce oscillatory behaviors, it appears that the system now possesses a limit cycle. Experimental results for a similar system yielded asymmetrical power outputs. Due to the sign-invariance of (1) with respect to  $x$ , it is not possible to obtain asymmetric solutions while assuming a uniform injection current and a symmetric lateral step index function. While either of these could yield an asymmetric solution, the former is of primary concern. Thus for this array, it is assumed that the largest injection current is in the first waveguide, with a linearly decreasing current in successive waveguides. The results of this assumption are shown in Fig. 2. The result is persistent oscillations that are nearly  $\pi$  out of phase, similar to those seen by Winful in the case of smaller arrays [2, 3]. New to these results are unequal injection currents and the impact they have.

Self-evident in Fig. 2 is the lack of symmetry typically found in these systems. This results in an unequal average power as well as an unequal amplitude of oscillations. However, the frequency of oscillation remains similar for the four waveguides that are above threshold. The fifth waveguide is clearly exhibiting different behavior. This is

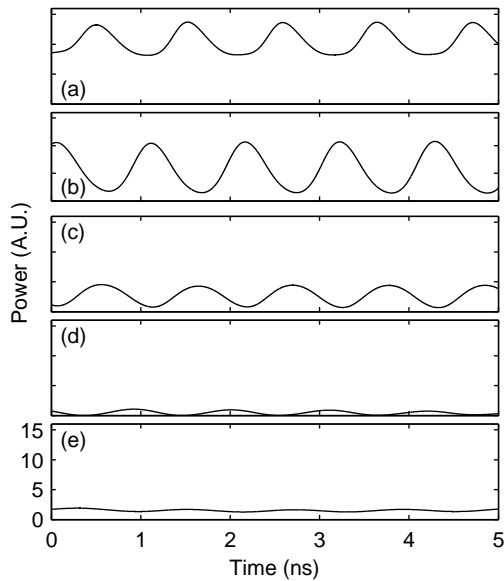


Figure 2: Numerical simulation of power fluctuations at 400 mA of injection current. The power output for emitters 1-5 are given in the plots labeled (a)-(e) respectively. The decrease in average power with respect to waveguide number is due to the slope of the injection current. The slope has altered both the average power and the amplitude of oscillation of each emitter.

due to the emitter barely exceeding the threshold current. The amplitude of oscillation can be controlled by changing the slope of the injection current or the separation between waveguides. Increases in both tend to decrease the amplitude of oscillations. That the system settles to a common frequency should be expected. In the absence of charge carrier dynamics, this would reduce to a relatively simple five-emitter dielectric waveguide problem which has been studied at length [11, 12]. In that problem, only a few of the modes are typically excited over the duration of the problem. The presence of the charge carriers couples these modes resulting in the temporal dynamics observed. Yet, as each supermode includes power in all five waveguides, it makes sense the oscillation frequency in each is roughly the same.

For a particular set of parameters matching experiment, the phase difference between waveguides remains fairly constant at  $\pi$  over injection currents ranging from 380 mA to 500 mA. The fundamental frequency of oscillation increases in that range from around 0.75 GHz to 1.5 GHz as shown in Fig. 3. In addition to the fundamental frequency, two higher harmonics are also visible, starting at 1.5 GHz and approximately 2.25 GHz respectively. These increase at roughly twice and three times the rate of the fundamental frequency, as one would expect from harmonics. There are also streaks of frequency components that exist between the harmonics. These streaks are neither at the proper frequency nor increase at the proper

rate to be harmonics. The dynamics of these streaks is a source of disagreement between numerics and experiment. In experiment, the fine structure crosses the fundamental frequency and harmonics. As shown in Fig. 3, these crossings do not occur. Apart from that, there is good qualitative and quantitative agreement between theory and experiment.

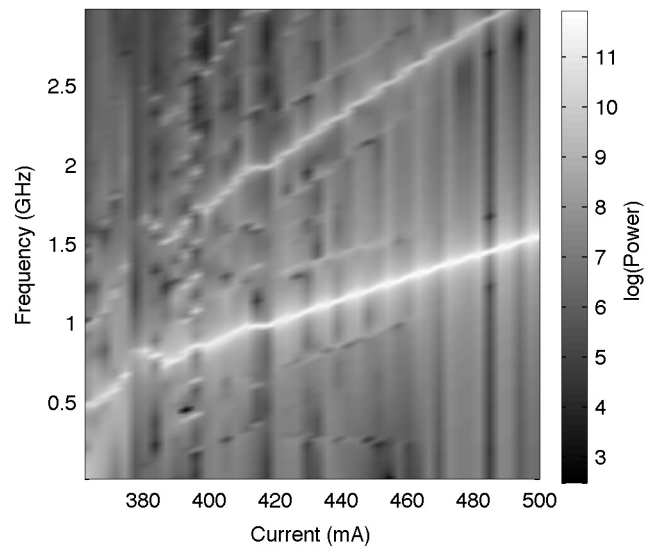


Figure 3: Frequency spectrum vs injection current obtained numerically. This matches the general pattern observed in experimental results with an increasing fundamental frequency of oscillation and higher harmonics. Additionally, there exists fine structure that appears between the harmonics.

In addition to the injection current, the frequency of oscillation is sensitive to a wide range of parameter values including the separation of the waveguides and the level of index guiding. Minor changes in these parameters tend to have a larger impact upon the resulting dynamics of the system. Indeed, altering the spacing of the waveguides from  $7 \mu\text{m}$  to  $9 \mu\text{m}$  results in the system changing from stable to oscillatory and then to chaotic behavior, traversing the entire range of potential behaviors. Even a shift of one waveguide is capable of altering the dynamics of the system. Therefore, between the combination of altering injection currents and individual waveguide separations it should be possible to achieve almost any desired oscillatory power output. The combination of the physical design of the waveguide array as well as the level of injection current provides a method for tuning the output of the array. Alterations in the structure of the array produce large scale changes in dynamics as shown by Winful [3], while changes in injection current produce relatively fine scale changes in the output frequency.

## 4 Conclusions

The output power dynamics of a five-emitter array have been analyzed and several different dynamical behaviors observed. While the stable out-of-phase, oscillatory, and chaotic behaviors have been achieved, the oscillatory behavior is of most interest as it lends itself to the production of all-optical GHz oscillators among other applications. Here, GHz frequency oscillation rates were achieved, with the fundamental frequency ranging from 0.75 GHz at 380 mA to 1.5 GHz at 500 mA. The second and third harmonics have two- and three-times the frequency respectively. Additionally, the output power between adjacent waveguides differs by a phase shift of approximately  $\pi$  that persists throughout the range of currents studied. It should be noted that these behaviors depend heavily upon the parameters chosen for the system and a wide range of potential behaviors exists. For instance, it is easy to obtain systems that are chaotic for almost all injection current values greater than the threshold. Indeed, the majority of parameter space yields undesirable behavior. Yet, with parameter values that are physically plausible for a five-emitter AlGaAs array, numerical results with good quantitative agreement to experimental results were obtained. The present limitations of this model include its inability to accurately capture the fine structure of the frequency components observed in experiment. While the fine structure is observed, it behaves differently than the structure seen in experiments. Due to the relatively low powers in those frequencies, and the decibel scale used in Fig. 3 the streaks have a minor impact on the resulting intensity dynamics. Therefore, the model accurately captures the intensity dynamics that occur, and thus can be used in the future as a design tool for such arrays.

## References

- [1] S. Wang and H. Winful, "Dynamics of phase-locked semiconductor laser arrays," *Appl. Phys. Lett.*, vol. 52, pp. 1774–1776, 1988.
- [2] L. Rahman and H. Winful, "Improved coupled mode theory for the dynamics of semiconductor laser arrays," *Optics Letters*, vol. 18, pp. 128–130, 1993.
- [3] L. Rahman and H. G. Winful, "Nonlinear dynamics of semiconductor laser arrays: a mean field model," *IEEE Journal of Quantum Electronics*, vol. 30, pp. 1405–1416, June 1994.
- [4] S.-S. Wang and H. G. Winful, "Propagation model for the dynamics of gain-guided semiconductor laser arrays," *J. Appl. Phys.*, vol. 73, pp. 462–464, January 1993.
- [5] B. Botez and G. Peterson, "Modes of phase-locked diode-laser arrays of closely spaced antiguides," *Electronics Letters*, vol. 24, pp. 1042–1044, Aug 1988.
- [6] J. Buus, "The effective index method and its application to semiconductor lasers," *IEEE Journal of Quantum Electronics*, vol. QE-18, pp. 1083–1089, July 1982.
- [7] G. P. Agrawal, "Lateral analysis of quasi-index-guided injection lasers: transition from gain to index guiding," *Journal of Lightwave Technology*, vol. LT-2, pp. 537–543, August 1984.
- [8] G. R. Hadley, "Transparent boundary conditions for the beam propagation method," *IEEE Journal of Quantum Electronics*, vol. 28, pp. 363–370, January 1992.
- [9] K. Kawano and T. Kitoh, *Introduction to Optical Waveguide Analysis: Solving Maxwell's Equations and the Schrodinger Equation*. John Wiley and Sons, 2001.
- [10] H. G. Winful, "Instability threshold for an array of coupled semiconductor lasers," *Phys. Rev. A*, vol. 46, pp. 6093–6094, Nov 1992.
- [11] M. J. Adams, *An Introduction to Optical Waveguides*. John Wiley and Sons, 1981.
- [12] A. Yariv, *Quantum Electronics, 3rd Edition*. Wiley, January 1989.